



Fermi National Accelerator Laboratory

FERMILAB-Pub-89/145-E

[E-715]

New Measurement of the Production Polarization and Magnetic Moment of the Cascade Minus Hyperon*

L. H. Trost^(a), E. R. McCliment, and C. R. Newsom
Department of Physics and Astronomy
University of Iowa
Iowa City, Iowa 52242

S. Y. Hsueh^(b), D. Müller, J. Tang, R. Winston, and G. Zapalac^(c)
Enrico Fermi Institute
The University of Chicago
Chicago, Illinois 60637

E. C. Swallow
Department of Physics
Elmhurst College
Elmhurst, Illinois 60126
and
Enrico Fermi Institute
The University of Chicago
Chicago, Illinois 60637

**J. P. Berge, A. E. Brenner^(d), P. S. Cooper, P. Grafström^(e),
E. Jastrzembski^(f), J. Lach, J. Marriner, R. Raja, and V. J. Smith^(g)**
Fermi National Accelerator Laboratory
Batavia, Illinois 60510

E. W. Anderson
Department of Physics
Iowa State University
Ames, Iowa 50011

**A. S. Denisov, V. T. Grachev, V. A. Schegelsky, D. M. Seliverstov,
N. N. Smirnov, N. K. Terentyev, I. I. Tkatch, and A. A. Vorobyov**
Leningrad Institute of Nuclear Physics
Leningrad, U.S.S.R.

P. Razis^(h), and L. J. Teig⁽ⁱ⁾
J. W. Gibbs Laboratory
Yale University, New Haven, Connecticut 06511
June 1989

*To be published in Phys. Rev. D



New Measurement of the Production Polarization and Magnetic Moment
of the Cascade Minus Hyperon

L. H. Trost^(a), E. R. McCliment, C. R. Newsom

Department of Physics and Astronomy, University of Iowa,
Iowa City, Iowa 52242

S. Y. Hsueh^(b), D. Müller, J. Tang, R. Winston, G. Zapalac^(c)

Enrico Fermi Institute, The University of Chicago,
Chicago, Illinois, 60637

E. C. Swallow

Department of Physics, Elmhurst College, Elmhurst, Illinois 60126,
and Enrico Fermi Institute, The University of Chicago
Chicago, Illinois 60637

J. P. Berge, A. E. Brenner^(d), P. S. Cooper, P. Grafström^(e), E.

Jastrzembski^(f), J. Lach, J. Marriner, R. Raja, V. J. Smith^(g)

Fermi National Accelerator Laboratory, Batavia, Illinois 60510

E. W. Anderson

Department of Physics, Iowa State University, Ames, Iowa 50011

A. S. Denisov, V. T. Grachev, V. A. Schegelsky, D. M. Seliverstov,

N. N. Smirnov, N. K. Terentyev, I. I. Tkatch, A. A. Vorobyov

Leningrad Nuclear Physics Institute

Leningrad, USSR

and

P. Razis^(h), L. J. Teig⁽ⁱ⁾

J. W. Gibbs Laboratory, Yale University, New Haven, CT 06511

PACS Number: 13.30.Ce

ABSTRACT

We have measured the production polarization and magnetic moment of a sample of 89K Ξ^- hyperons produced in the inclusive reaction $p(400 \text{ GeV}/c) + \text{Cu} \rightarrow \Xi^- + X$. The weighted average of the polarization is $-0.070 \pm 0.008 \pm 0.010$ at a p_t of $0.63 \text{ GeV}/c$. The Ξ^- 's magnetic moment yields the value $\mu_{\Xi} = -0.661 \pm 0.036 \pm 0.036$ nuclear magnetons. The first error is statistical, the second systematic.

The experimental values of baryon magnetic moments provide a sensitive means to test the various quark models of elementary particles. Previous measurement of the cascade's magnetic moment by Rameika *et al.* disagreed with the predictions of the naive quark model, prompting many refinements of the model.¹⁻² In this work we present new measurements of the cascade production polarization and magnetic moment from data collected in experiment E715 at Fermilab.³

In this experiment a secondary beam containing a 0.5% admixture of Ξ^- with an average momentum of approximately 250 GeV/c was inclusively produced by collisions of 400 GeV/c protons on a copper target. The Ξ^- polarization was determined from a set of events containing the decay chain $\Xi^- \rightarrow \Lambda^0 + \pi^-$ followed by $\Lambda^0 \rightarrow p + \pi^-$. These events were selected from a sample containing only charged particles in the final state.

Parity conservation requires the Ξ^- polarization to be normal to the production plane (parallel or antiparallel to the vector product $\mathbf{p}_{\text{inc}} \times \mathbf{p}_{\Xi}$, where \mathbf{p}_{inc} is the momentum of the incident proton and \mathbf{p}_{Ξ} the momentum of the Ξ^- .) By convention positive polarization is in the direction of positive cross product. The targeting angle θ_t between the incident proton and the Ξ^- can be varied by means of dipole magnets upstream of the target. Data was taken with the production plane both horizontal (horizontal targeting) and vertical (vertical targeting).⁴ In each production mode two different targeting angles were selected. For vertical targeting these angles were +3.07 and -2.01 mrad with an average secondary beam momentum of

244.7 GeV/c. For horizontal targeting the angles were +2.10 mrad with momentum 237.5 GeV/c and -3.06 mrad with momentum 253.5 GeV/c.

The E715 apparatus is described in detail in Reference 3. The parts relevant to this experiment along with a superimposed E^- decay chain are shown schematically in Figure 1. They include the following: the three magnets M_1 , M_2 , and M_3 ; the system of proportional wire chambers (PWC); drift chamber clusters A, B, and C; and the various scintillators used in the trigger. Magnet M_1 has a length of 7.3 m and a field integral of 17.6 T·m, giving a bend angle of 21 mrad at a momentum of 250 GeV/c. The PWC's are used in conjunction with this magnet to measure the momentum of the E^- prior to its decay. The calibration and resolution of the PWC system is discussed in detail in Reference 3. Overall the momentum resolution of the secondary beam is $\Delta p/p = \pm 0.7\%$ (1σ).

The momenta of the decay products are measured by a downstream spectrometer consisting of magnets M_2 and M_3 and drift chamber clusters A, B, and C. Clusters A and B and magnet M_2 determine the momentum of the pions and, in conjunction with magnet M_3 and cluster C, the proton momentum. Overall, the downstream spectrometer has the following resolution for both pions and protons: $\Delta(1/p) = 0.0004$ (GeV/c) $^{-1}$, $\Delta\theta = 150$ μ rad (azimuth), and $\Delta\phi = 50$ μ rad (dip). The momentum distributions measured by the downstream spectrometer are in agreement with Monte Carlo studies using our 3-prong cascade decay hypothesis.

The entire system is aligned using beam tracks with the magnets off. The magnets M_2 and M_3 have been calibrated previously; they impart a known transverse momentum p_t , which is approximately 0.8 GeV/c. As a check on the consistency of the calibration we demand overall momentum conservation in the mean, and the invariant mass distributions (Figure 2) that we use for event selection must be centered on the accepted masses of the Λ^0 and Ξ^- .⁵

The trigger for cascade decays with three charged tracks in the final state consists of an upstream beam trigger, a negative track scintillator SC1, a positive track scintillator SC2, and a downstream beam veto. The raw data sample satisfying the trigger requirement contained approximately 4×10^6 events. The final Ξ^- decay sample was obtained as follows: First events were selected that have a beam track and at least two negative tracks and one positive track downstream. The reconstruction of a Λ^0 using two downstream tracks, one positive and one negative, was then required of these events. Next the reconstruction of a Ξ^- from a second downstream negative track not associated with the Λ^0 and the upstream beam track was required. At this stage only loose cuts of ± 30 MeV on either mass were imposed. The invariant mass distributions in Figure 2 are centered on the expected values (see Reference 5) and fall within the specified cuts. The final set of events were then required to pass the following cuts:

1. The Ξ^- and Λ^0 decay vertices must occur within a 14 m fiducial region located between the last chamber of PWC and the first

drift chamber of cluster A.

2. The Λ^0 decay vertex must be downstream of the Ξ^- decay vertex by at least 1σ (1 m).
3. An opening angle cut of $50 \mu\text{rad}$ was imposed on the downstream tracks to conform to the 2-particle resolution of the drift chambers.
4. The cuts on the invariant masses were tightened to $\pm 20 \text{ MeV}$.

Ambiguities were resolved as follows: If the event contained more than the requisite two negative tracks (15% of events) the best fit to the mass of the corresponding hyperon was used. If the same pion fit both the cascade and lambda hypotheses, we used the vertex to distinguish them provided the vertices were separated by more than 1σ ($\pm 1.0 \text{ m}$). Events were dropped if we could not resolve the ambiguity ($< 0.2\%$ of the events). Monte Carlo studies using this procedure reproduce the input polarization within the statistical error (1σ). The final vertical targeting data sample, after all the cuts, contained 22K events at each targeting angle. The horizontal targeting sample contained 25K events at $+2.1 \text{ mrad}$ and 20K events at -3.1 mrad .

In the center of momentum system (COM) of the Ξ^- the angular distribution of the pion daughter is given by

$$\frac{dW(\pm)}{d(\cos \theta_1)} = A_1(\cos \theta_1)(1 \mp \alpha_{\Xi} P_{\Xi 1} \cos \theta_1) \quad (1)$$

where $i = x, y, \text{ or } z$, $\cos \theta_i$ are the components of a unit vector in the pion's momentum direction, $A_i(\cos \theta_i)$ are the acceptance functions of the apparatus, and α_{Ξ} is the asymmetry parameter of the Ξ^- . The upper (lower) sign is for a positive (negative) targeting angle (reversing the targeting angle reverses the direction of the polarization.) A similar relation holds for the Λ^0 decay pion in the Λ^0 COM with the following replacement:⁶

$$\alpha_{\Lambda} \rightarrow \alpha_{\Xi}^{\text{eff}} = \alpha_{\Lambda}(1 + 2\gamma_{\Xi} - \alpha_{\Xi}^2)/3 \quad (2)$$

where γ_{Ξ} in this expression is another of the Ξ^- 's asymmetry parameters (see Reference 5). This means we can obtain a separate measurement of the cascade polarization from each decay mode, which provides us with the possibility of checking the consistency and systematic error of our measurements. To extract the polarization we exploit the sign reversal in Equation 1. We form the difference over the sum of two angular distributions, each having the form of Equation 3, but one with positive targeting angle, the other negative. Then the acceptance function cancels, giving the result⁷

$$\frac{\frac{dW(+)}{d(\cos \theta_i)} - \frac{dW(-)}{d(\cos \theta_i)}}{\frac{dW(+)}{d(\cos \theta_i)} + \frac{dW(-)}{d(\cos \theta_i)}} = -\alpha_{\Xi} P_{\Xi i} \cos \theta_i \quad (3)$$

Figure 3 shows the angular distributions for both vertical and horizontal targeting data obtained from this equation. The experimental points are determined from the individual $\cos \theta$ distributions in accordance with the left-hand side of Equation 3. The $F_i^{(\pm)}$ are the fractional numbers of events in each bin of the individual $\cos \theta$ distributions for positive (negative) targeting angles. The solid lines are 1-parameter fits to the right hand side of this equation.⁸ The slope of each straight line in Figure 3 is the corresponding product $\alpha_{\Xi} P_{\Xi i}$. The values of α_{Ξ} and other asymmetry parameters used in the calculation of $\alpha_{\Xi}^{\text{eff}}$ are taken from Reference 5: $\alpha_{\Xi} = -0.455 \pm 0.015$, $\gamma_{\Xi} = 0.89 \pm 0.008$, and $\alpha_{\Lambda} = 0.642 \pm 0.013$. With these values taken from the literature the slopes determine the polarization. The polarization components obtained in this manner are listed in Table 1 along with the reduced chi-squares for the fits. The final results are found in the rows marked "Best Fit". These values are obtained by fitting the angular distributions of both decay pions simultaneously.

The Ξ^- polarization is produced perpendicular to the production plane, and the field of magnet M_1 is vertically downward (-y direction.) With horizontal targeting the initial polarization is parallel to the magnetic field and there is no precession, whereas with vertical targeting the polarization is produced along the x axis and precesses about the y axis. Upon emerging from the magnet the x and z components of polarization must therefore be zero for horizontal targeting, and the y component must be zero for vertical

targeting. However, it will be noted that there is a 2σ discrepancy between the values of the x component of polarization in the vertical targeting case. We have studied this discrepancy, and, to the best of our knowledge, it is a statistical fluctuation. The best values of the polarization components in Table 1 obtained by an overall fit to both cascade and lambda decay are consistent with these requirements. This is supported by the opposite signs of P_x and P_y obtained from vertical and horizontal targeting, respectively (see Reference 4). Our best value of the cascade polarization, obtained from a weighted average of the horizontal and vertical targeting data is $P_{\Xi} = -0.070 \pm 0.008 \pm 0.010$. This value is plotted in Figure 4 along with values taken from Reference 1 for comparison.

The magnetic moment is determined from the precession of the polarization. For vertical targeting the angle of precession ξ is $\tan^{-1}(P_z/P_x)$. The g factor is related to the precession angle (in degrees) as follows:

$$\xi = -(13.0 \text{ deg/T}\cdot\text{m})(g/2 - 1)\int B dl \quad (4)$$

and the magnetic moment is

$$\mu_{\Xi} = -g\mu_N m_P / (2m_{\Xi}) \quad (5)$$

where μ_N is the nuclear magneton. The $\int B dl$ of magnet M_1 in Equation 3 is inferred from the bend angle and the calibration procedure. It has the value 17.3 T·m. Using this value and combining Equations 3 and 4 yields the results for the cascade magnetic moment listed in Table 2. This table gives the values obtained from the Ξ^- and Λ^0 decay pions separately and a best value obtained from a simultaneous fit to both decays. Using the best value and including systematic error (discussed below) our result for the magnetic moment is $\mu_{\Xi} = -0.661 \pm 0.036 \pm 0.036$. The first error is statistical, the second systematic. This result is consistent with the result, -0.69 ± 0.04 , quoted in Reference 1. Moreover, our field integral is significantly different from theirs. The combined results are thus free of multiple 360° ambiguities (multiple 180° ambiguities are resolved by the horizontal targeting results.)

The systematic error was determined by studying the change in the results affected by varying the Λ^0 and Ξ^- mass cuts, the fiducial volume cut, and the opening angle cut. In addition the beam momentum distribution was divided into 6 subsamples with roughly equal numbers of events and the polarization components determined for each subsample. In no case did any measured component of the cascade production polarization vary by more than the statistical error at the 1σ level. The systematic error for the magnetic moment was deduced from that of the polarizations.

We are grateful to the Fermilab staff, particularly the Proton, Physics, and Computing Departments, for their assistance. This work

was supported in part by the U.S. Department of Energy under Contracts No. DE-AC02-87ER40318, No. DE-AC02-80ER10587, No. DE-AC02-76C H03000, and No. DE-AC02-76ER03075, and by the USSR Academy of Sciences.

(a) Submitted in partial fulfillment of the requirements of the M.S. degree at the University of Iowa.

(b) Present address: Fermilab.

(c) Present address: Stanford Linear Accelerator Center, Stanford, CA 94305.

(d) Present address: Supercomputer Research Center, Institute for Defence Analyses, 4380 Forbes Blvd., Lanham, MD 20706.

(e) Present address: E.P. Division, CERN, CH-1211 Geneva 23.

(f) Present address: Brookhaven National Laboratory, Upton, Long Island, NY 11973.

(g) Permanent address: H.H. Wills Physics Laboratory, University of Bristol, Bristol BS8 1TL, England.

(h) Present address: Eidg. Technische Hochschule, Zurich, Switzerland.

(i) Present address: Mitre Corporation, Bedford, MA 01730.

REFERENCES

1. R. Rameika, *et al*, Phys. Rev. Lett. 52, 581 (1984).
2. A. De Rujula, H. Georgi, and S. L. Glashow, Phys. Rev. D 12, 147 (1975). For a review of theoretical work through 1983, see A. J. G. Hey, R. L. Kelly, Phys. Repts 96, 73 (1983).
3. S. Y. Hsueh, *et al.*, Phys Rev D 38, 2056 (1988). A complete description of the apparatus, its calibration, and resolution is found in this paper.
4. The coordinate system is right handed with z along the direction of the cascade momentum and x horizontal, putting y in the vertical plane. With a positive horizontal targeting angle $p_{inc} \times p_{\Xi}$ is along the negative y axis, whereas a positive vertical targeting angle puts this vector along the positive x axis. Thus, in the absence of precession, a positive x component of polarization from vertical targeting corresponds to a negative y component from horizontal targeting. For each event the coordinate axes rotate in the magnet so that the z axis remains parallel to the cascade momentum, while the x axis remains horizontal. The precession of the polarization is thus measured relative to the momentum.
5. Particle Data Group, Phys. Lett. B204, 1 (1988)

6. S. Gasiorowicz, Elementary Particle Physics, Wiley, New York, 1966.
7. In our case the targeting angles are not equal and opposite. However, the acceptance still cancels, and one obtains the average of the polarizations at the two targeting angles plus a small nonlinear term that is proportional to the difference of the polarizations. Our results are not sensitive enough to detect the nonlinearity.
8. Before doing the 1-parameter fit, a 2-parameter fit was done with the $\cos \theta$ distributions folded in half. After ascertaining that the intercept at $\cos \theta = 0$ was consistent with 0, the 1-parameter fit was done. Both fits give $\chi^2/\text{DOF} \approx 1$.

Table 1. Cascade Polarization Components.[†]

Horizontal Targeting

	X	Y	Z
From π_A	0.008 ± 0.017 (0.85)	0.104 ± 0.017 (1.24)	-0.031 ± 0.018 (1.06)
From π_E	-0.014 ± 0.021 (1.23)	0.064 ± 0.019 (0.94)	-0.009 ± 0.022 (1.03)
Best Fit	0.002 ± 0.013 (0.66)	0.082 ± 0.012 (0.52)	-0.022 ± 0.014 (1.08)

Vertical Targeting

	X	Y	Z
From π_A	-0.079 ± 0.015 (0.81)	0.006 ± 0.014 (1.08)	0.008 ± 0.016 (0.91)
From π_E	-0.024 ± 0.018 (1.38)	-0.011 ± 0.017 (0.90)	0.026 ± 0.019 (1.01)
Best Fit	-0.057 ± 0.011 (1.23)	-0.001 ± 0.011 (0.93)	0.016 ± 0.012 (0.85)

[†]. The numbers in parentheses are the χ^2/DOF . The errors are statistical.

Table 2. Summary of the precession angle and the magnetic moment measurements from vertical targeting data.

	ξ (rad)	$\frac{g}{2} - 1$	μ_E (μ_N)
From π_A	-0.101 ± 0.20	-0.025 ± 0.051	-0.692 ± 0.036 (0.85)
From π_E	-0.825 ± 0.52	-0.206 ± 0.135	-0.564 ± 0.094 (0.96)
Best Fit	-0.274 ± 0.20	-0.069 ± 0.052	-0.661 ± 0.037 (0.92)
Reference 1			-0.69 ± 0.04

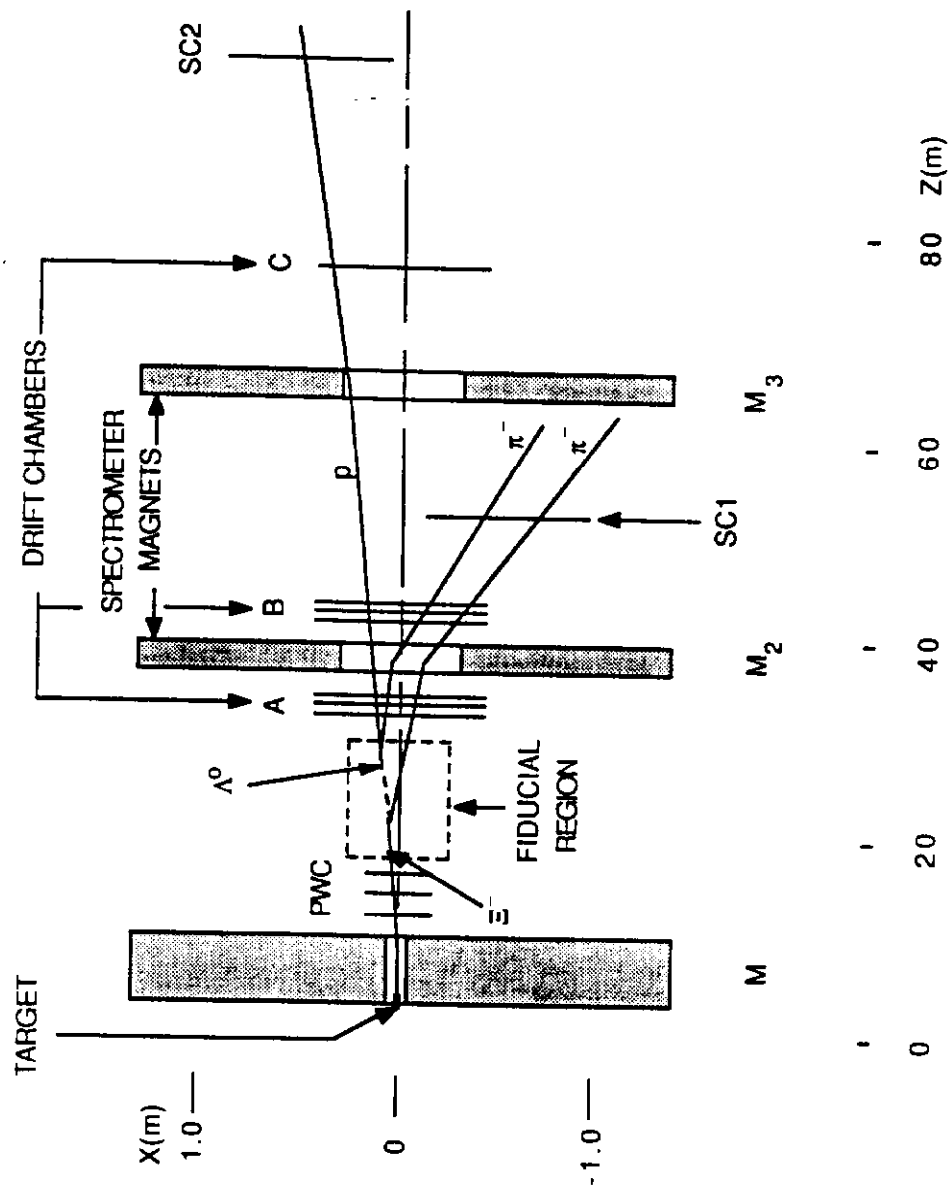


Figure 1. Experimental apparatus.

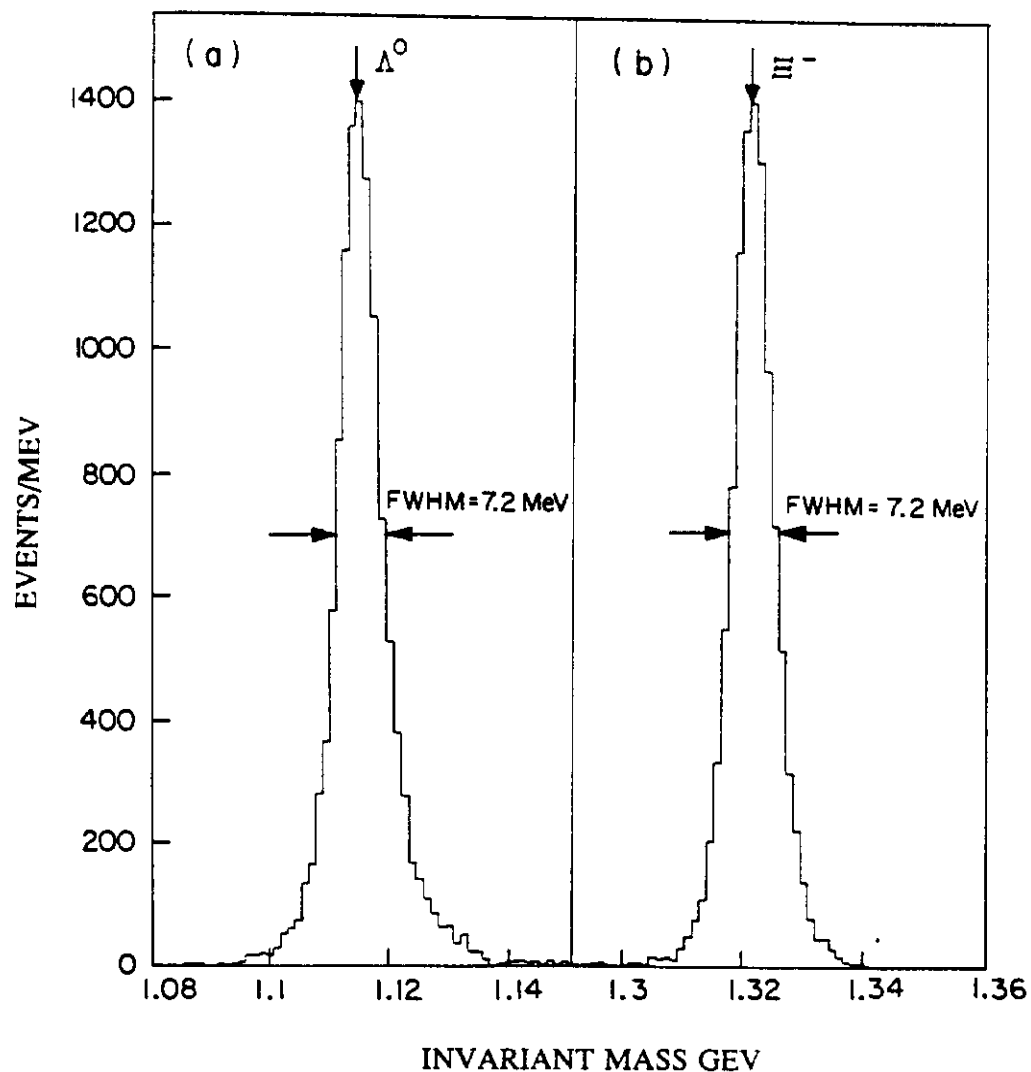


Figure 2. Invariant mass spectra. (a) Uses hypothesis that positive and negative downstream tracks are proton and π^- , respectively. Peak is centered on Λ^0 mass indicated by the vertical arrow. (b) Uses hypothesis that the decay products of beam particle are Λ^0 and π^- . Peak is centered on Ξ^- mass.

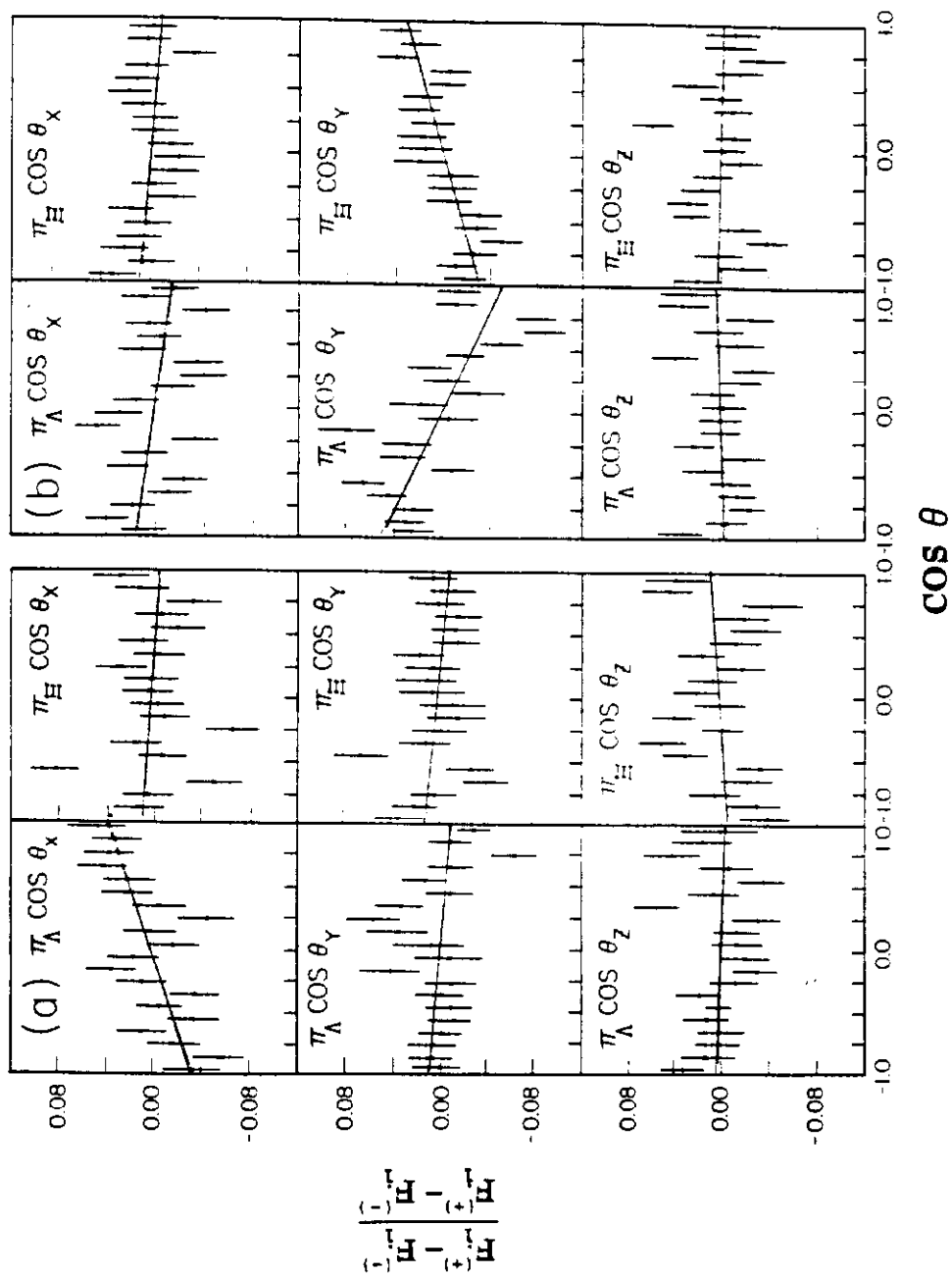


Figure 3. Experimental angular distributions of decay pions.
 (a) Vertical targeting. (b) Horizontal targeting. The solid lines represent a 1-parameter least-squares fit to the experimental points.

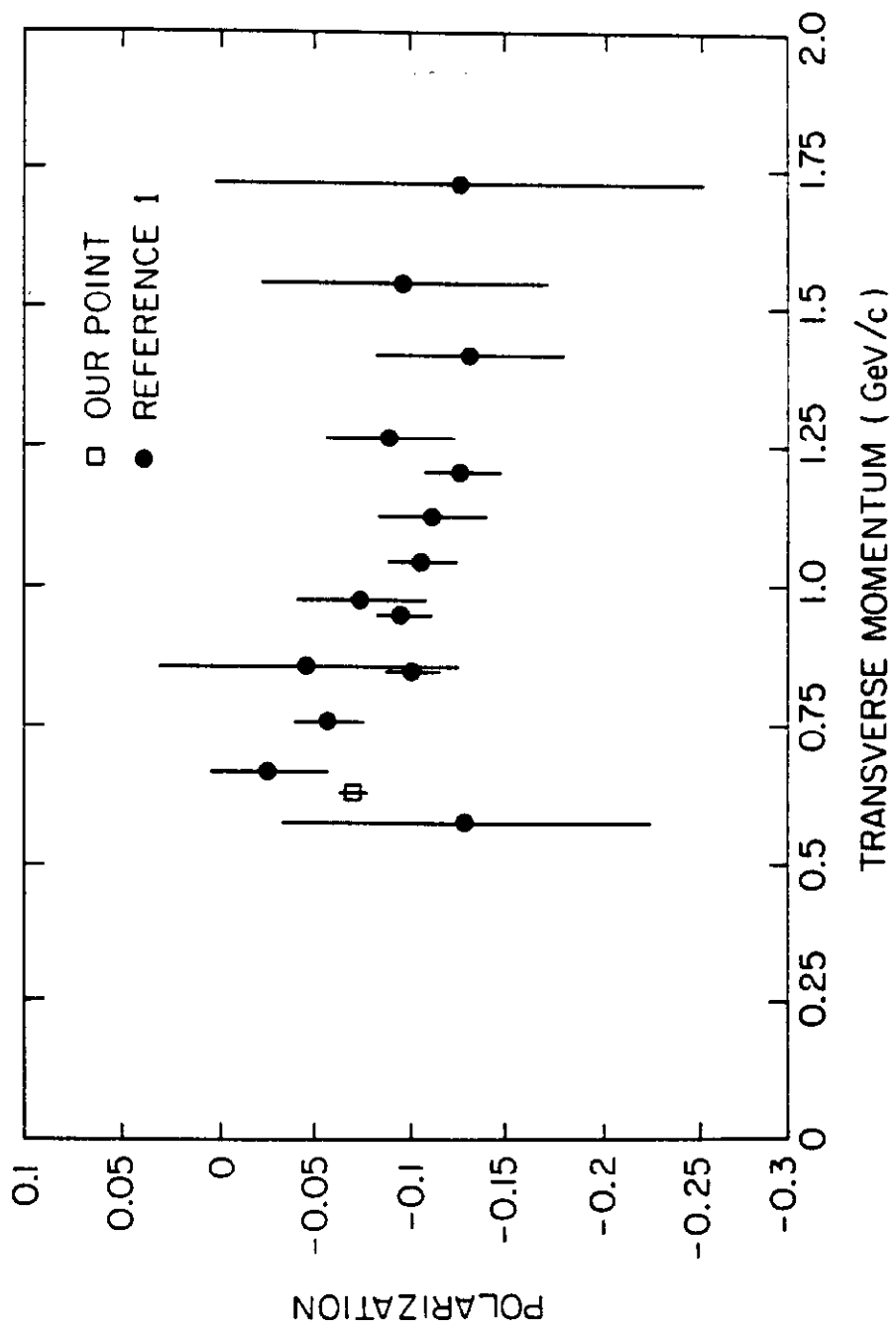


Figure 4. Cascade polarization vs. transverse momentum.